



## Full Text View

[Volume 30, Issue 8 \(August 2000\)](#)

### Journal of Physical Oceanography

Article: pp. 2055–2071 | [Abstract](#) | [PDF \(1.51M\)](#)

## Transport Properties in the Adriatic Sea as Deduced from Drifter Data

**Pierpaolo Falco**

*Instituto Universitario Navale, Naples, Italy*

**Annalisa Griffa**

*RSMAS, University of Miami, Miami, Florida, and IOF-CNR, La Spezia, Italy*

**Pierre-Marie Poulain**

*Naval Postgraduate School, Monterey, California*

**Enrico Zambianchi**

*Instituto Universitario Navale, Naples, Italy*

(Manuscript received March 9, 1999, in final form October 6, 1999)

DOI: 10.1175/1520-0485(2000)030<2055:TPITAS>2.0.CO;2

### ABSTRACT

The surface transport properties in the Adriatic Sea, a semienclosed subbasin of the Mediterranean Sea, have been studied using a drifter dataset in the period December 1994–March 1996. Three main points have been addressed. First, the exchange between southern and northern regions and between deep and coastal areas have been studied, focusing on the role of topography. A significant cross-topography or cross-shelf exchange has been found, probably due to the direct wind forcing and to the influence of stratification that isolates the surface flow from bottom effects, especially in the open sea. Second, a Lagrangian transport model with parameters derived from the data has been implemented. Simulated particles have been compared with drifter data with positive results. The model is found to be able to reproduce reality with good approximation, except for a specific advective event during the late summer season. Finally, the residence timescale  $T$ , that is, the average time spent by a surface particle in the basin, has been estimated. Direct estimates from the data suggest  $T \approx 70$ – $90$  days, but these values are biased due to the finite lifetime of the drifters. Model results have been used to estimate the bias, and they suggest a “true” value of  $T \approx 200$  days.

#### Table of Contents:

- [Introduction](#)
- [Background](#)
- [General transport properties](#)
- [A transport model applied](#)
- [Estimates of residence](#)
- [Discussion and conclusions](#)
- [REFERENCES](#)
- [APPENDIX](#)
- [TABLES](#)
- [FIGURES](#)

#### Options:

- [Create Reference](#)
- [Email this Article](#)
- [Add to MyArchive](#)
- [Search AMS Glossary](#)

#### Search CrossRef for:

- [Articles Citing This Article](#)

## 1. Introduction

Transport by ocean currents is known to be extremely effective in controlling the distribution of water mass properties on a broad range of scales, from the global ocean basin scale (thousands of kilometers) to the microscale (centimeters). On the global scale, for instance, ocean transport of heat and salt plays a key role in the earth's climate. In the coastal zone and semienclosed seas, transport by basin-scale and mesoscale current features is even more crucial due to the diversity of flotsam and jetsam (from pollutants to debris of different origin, even to men at sea) encountered in the vicinity of populated coasts and the complexity of the local ecosystems.

The Adriatic Sea, a landlocked semienclosed basin in the northern Mediterranean, is a region characterized by strong gradients in water properties (temperature, salinity, nutrients, pigment concentration, etc.) due to the important surface (air-sea) and lateral (river runoff and strait exchange) fluxes; transport and fluid exchange processes are therefore of paramount importance.

In this paper, we study the transport properties in the Adriatic Sea using a surface drifter dataset collected during the period December 1994–March 1996. Drifters are considered to be quasi-Lagrangian instruments because they do not perfectly follow the water particles due to wind/wave-induced slippage and due to the fact that they are constrained to move at the surface. In good approximation, however, they follow rather well the horizontal surface currents and can be thus viewed as surface passive tracers. In this sense, they are optimal instruments with which to study horizontal surface currents and the associated transport on a broad range of scales (including the predominant basin and mesoscales) over the entire basin.

The drifter dataset used in this work has already been presented in previous papers ([Poulain 1999](#); [Poulain and Zanasca 1999](#)), where the structure of the mean circulation and the subtidal velocity variability were quantitatively described. In the present work, we use the same drifter observations to estimate simple and useful transport properties of the surface circulation in the Adriatic.

Because of the data distribution, the results are mainly relevant to the southern and central parts of the basin and are mostly representative of the year 1995. We focus on three main points.


1. The description of transport properties for particles entering the basin through the Strait of Otranto, the Adriatic southern entrance. In particular, we explore the exchange between southern and northern regions and the role of topography in the exchange between deep and coastal regions.
2. The use of a simple transport model (advection–diffusion like) where the flow is decomposed in mean flow and eddy field, to investigate the tracer behavior at the surface.
3. The estimation of the residence time, that is, the average time spent in the basin, for particles launched at the Strait of Otranto.

These points have direct applications to the study of biological or chemical processes in the Adriatic ([Gacic et al. 1999](#)). They are also important for coastal zone management and possibly for search-and-rescue operations.

The work is organized as follows. A brief review of the Adriatic Sea oceanography and the characteristics of the dataset is given in [section 2](#), together with a synthesis of the basic statistical results on the general circulation. In [section 3](#), the drifter data are used to study the transport properties, while the flow decomposition and the transport model are presented and compared to the drifter-inferred results in [section 4](#). The basin residence time is studied in [section 5](#).

## 2. Background

### *a. The Adriatic Sea*

The Adriatic Sea ([Fig. 1a](#) ) is an elongated (about 800 km by 200 km) semienclosed basin connected to the rest of the Mediterranean at its southern entrance through the Strait of Otranto. It can be divided into three parts: The northernmost region is shallow with a gentle slope reaching depths of about 100 m at the latitude of Ancona. Farther south, the topography drops quickly to more than 200 m in the Jabuka Pit in the central part. This region is separated from the third and deepest part by the Palagruza Sill. The southern Adriatic is characterized by a deep at its center, the South Adriatic Pit, reaching 1200-m depth. The bottom rises again to a maximum sill depth of 780 m in the 75-km-wide Strait of Otranto. In this work,

Search Google Scholar for:

- [Pierpaolo Falco](#)
- [Annalisa Griffa](#)
- [Pierre-Marie Poulain](#)
- [Enrico Zambianchi](#)

the exact limits of the three subbasins are taken following [Artegiani et al. \(1997a\)](#). They are shown in [Fig. 1a](#) together with the boundary at 40.4°N in the Strait of Otranto taken as the entrance of the Adriatic. Note that these definitions, especially the limit defining the northern subbasin, may differ from others found in the literature.

Historical hydrographic and moored current meter data ([Orlic et al. 1992](#); [Artegiani et al. 1997a](#)) and recent drifter measurements ([Poulain 1999](#)) indicate that the mean surface circulation of the Adriatic consists of a basinwide cyclonic gyre with a northwestward flow along the eastern side (Albanian and Croatian coasts) and a southeastward return flow along the Italian coast on the western side. The latter flow, named the Western Adriatic Current, is one of the most prominent circulation features of the Adriatic. Several smaller circulation cells are embedded in this large-scale gyre, such as the quasi-permanent cyclonic gyre in the southern part around the South Adriatic Pit. The northwestward flowing water on the eastern side tends to turn cyclonically around the Jabuka Pit in the central region and also farther north near the latitude of the Po River delta and joins the southeastward return current.

The global Adriatic circulation system is modulated seasonally. For instance, in winter the northward currents on the eastern side are wider and more pronounced. In summer, the southward currents along the Italian coast predominate ([Buljan and Zore-Armanda 1976](#); [Artegiani et al. 1997b](#)). The main circulation patterns are constantly perturbed by high-frequency current variations at inertial/tidal scales and mesoscales. In particular, the wind stress is an important driving mechanism, causing transient currents that can be an order of magnitude larger than the mean circulation. For example, the bora winds (blowing from the northeast) induce pronounced transient currents in the northern Adriatic ([Zore-Armanda and Gacic 1987](#)) and trigger upwelling events near the eastern coast of the central and southern Adriatic ([Bergamasco and Gacic 1996](#)). Tidal currents are mostly important at the head of the basin in the northern Adriatic with amplitudes reaching about  $15 \text{ cm s}^{-1}$  ([Buljan and Zore-Armanda 1976](#)). The runoff of freshwater from rivers also influences the surface circulation substantially. In the northern Adriatic, the shelf area along the western coast is dominated by the Po River outflow, which in winter remains mostly confined to a coastal boundary layer whereas in summer it spreads farther offshore in a cross-basin direction ([Malanotte-Rizzoli and Bergamasco 1983](#)). In summer, the Po freshwater runoff is the major forcing mechanism of the Western Adriatic Current ([Artegiani et al. 1997b](#)).

### *b. The drifter data*

Starting in December 1994, 62 surface drifters were deployed in the Adriatic Sea and in the Strait of Otranto as part of the NATO SACLANT Otranto Gap project ([Poulain and Zanasca 1998](#); [Poulain 1999](#)). The majority of them (52) were deployed on the eastern side of the Strait of Otranto in five distinct episodes from December 1994 to October 1995. Clusters of 7 to 15 drifters were deployed at fixed locations in the strait ([Table 1](#)). In addition, 10 drifters were released in the northern and central Adriatic in May 1995.

Here we concentrate on the drifter dataset inside the Adriatic Sea ([Fig. 1b](#)), defined as north of 40.4°N ([section 2a](#)). Of the 52 drifters launched in the Strait of Otranto, only 31 entered the Adriatic Sea and survived more than a few days. The considered dataset includes these 31 drifters plus the 10 drifters released inside the basin, for a total of 41 drifters. The observation time spans the period between 4 December 1994 and 23 March 1996. [Table 1](#) presents more information on the deployment episodes in the Strait of Otranto, including the time periods at which the drifters entered the Adriatic by crossing latitude 40.4°N.

Most of the drifters were similar to the ones used in the Coastal Dynamics Experiment (CODE) in the early 1980s ([Davis 1985](#)). Details on the drifter hardware are given in [Poulain \(1999\)](#) and [Poulain and Zanasca \(1998\)](#). The drifter system extends within the first meter of water. Comparison with current meter measurements ([Davis 1985](#)) and studies using dye to measure relative water movements showed that the CODE drifter-inferred velocities are accurate to about  $3 \text{ cm s}^{-1}$ , even during strong wind conditions. The drifters were tracked by the Argos system onboard the NOAA polar-orbiting satellites. For the latitude range of the Adriatic Sea, the typical number of good drifter positions per day was eight using two satellites. The raw position data were despiked using statistical and manual techniques described in [Poulain and Zanasca \(1998\)](#). Optimal interpolation or “kriging” ([Hansen and Poulain 1996](#)) was then applied to the time series to obtain regularly sampled data at 2-h intervals. Velocity components were estimated from centered finite differences of the interpolated positions. The interpolated position and velocity time series were subsequently low-pass filtered (designed filter with cutoff period of 36 h) and were subsampled at 6-h intervals. Based on the typical Argos location accuracy and the characteristics of the above averaging/filtering, we estimated the low-pass filtered velocity accuracy to be  $2\text{--}3 \text{ cm s}^{-1}$ .

The drifter lifetimes range from 0 to 220 days over the whole dataset ([Poulain 1999](#)), the end of transmission being due to various reasons such as battery failure, grounding, or being picked up. The drifter mean half-life in the Adriatic, that is, the time after deployment for which 50% of the drifters still provide useful data, is about 100 days.

### *c. Mean flow and variability*

Before discussing the transport properties in the Adriatic, we briefly review the characteristics of its surface circulation as revealed by the drifter dataset (Poulain 1999). The velocity estimates were averaged in bins of  $0.25^\circ$  latitude by  $0.25^\circ$  longitude to obtain estimates of the large-scale mean circulation during the measurement period. The size of the bins was chosen so as to resolve as well as possible the subbasin mean circulation, yet keeping it large enough to have a substantial number of observations in the bins and assure robust results. This size is larger than the typical first internal Rossby radius of deformation in the Adriatic (Grilli and Pinardi 1998). Thus, most of the mesoscale eddy activity is averaged out. Notice that the data distribution is strongly nonuniform, both in space and in time. For example, no data were obtained in April 1995. Some of the domains in the northern and central subbasins were not sampled by any drifters (Fig. 1b). The inhomogeneity of the distribution results from the fact that most drifters entered the basin through the Strait of Otranto. This can introduce a bias in the mean flow circulation, especially where the data density gradients are large (Davis 1991).

The mean flow map of Poulain (1999) is reproduced in Fig. 1c, discarding the bins with less than 20 observations corresponding to 5 drifter days. In this way only the more significant statistics are considered. The mean flow is generally cyclonic, with marked closed recirculation in the southern and central subbasins, suggestive of the topographic influence on the flow. The circulation in the northern subbasin is not well resolved due to the low data density. In the following, we will concentrate on the central and southern subbasins only. Maximum mean flow speeds are found along the coastal boundaries with values reaching  $33 \text{ cm s}^{-1}$  near the Croatian coast.

The distribution of the variance (not shown here; see Poulain 1999) shows that the current variability is higher near the coasts where the mean currents are stronger. A maximum variance of approximately  $400 \text{ cm}^2 \text{ s}^{-2}$ , corresponding to  $20 \text{ cm s}^{-1}$  rms, is found. The velocity variance is generally not isotropic. Where the mean and rms currents are strong, they tend to be aligned with each other and parallel to the coastline. Most of this anisotropic variability is associated with current reversal events forced by the winds (Poulain 1999). It is important to stress that the velocity variance as defined here contains the spatial variability within the bins at scales smaller than 20–30 km and the temporal variations at meso-, synoptic, and seasonal scales. Some interannual signal might even be included, especially in the well-populated southern subbasin.

All the above results provide information on the mean circulation during the measurement period. Even though seasonal fluctuations are expected to be significant, the data coverage is not sufficient at this point to consider the various seasons separately.

### 3. General transport properties

Lagrangian data are especially suitable to study transport processes since they move with the currents following closely the motion of water parcels, at least at the large- and mesoscale (see above, section 2b). In this section, we focus on the characterization of the transport of passive tracers entering the Adriatic Sea through the Strait of Otranto and in particular on the role of topography in regulating exchanges between different regions. The analysis is performed using the 31 surface drifters entering the Strait of Otranto. It is worth underlining that, due to the finite lifetime of the drifters, the information we obtain is only relative to approximately the first 100 days of transport.

A first, qualitative idea of the behavior of surface water parcels flowing in the basin is given by the drifter trajectories. The variability, even within each drifter deployment, is high, and very different types of trajectories can be observed (Fig. 2). Some of the drifters initially recirculate (Fig. 2a) in the Strait of Otranto and at the basin entrance. Once definitely inside, some stay in the southern and central basins, recirculating or being trapped in the gyre region (Figs. 2a,b).

Some others are caught in strong coastal currents and move northward, eventually reaching the northern region (Fig. 2c). In particular, of the 31 drifters entering the Adriatic basin, 8 reached the northern basin, suggesting a significant exchange of surface water between the two regions (Table 1). The average time it takes drifters to reach the northern region is 80 days, with a standard deviation of 30 days (the high value of the latter is mainly due to two drifters deployed in late August, whose velocities were much higher than the other 6). It is worth mentioning that, using hydrographic data, Gacic et al. (1999) estimated an exchange over the whole water column of 20% in winter and 7% in summer between the two regions. Our results suggest a higher average exchange, but this has to be expected given that our results are only relative to the surface flow, while the results from Gacic et al. (1999) refer to the entire water column. Moreover, our statistics for the meridional exchange are based on a very limited number of drifters, a subset of which, as mentioned below, might represent an anomalous advection event.

Most of the northern passages (six over eight) occur for drifters launched in late August and in October (see Table 1), indicating that the exchange is enhanced during the late summer–fall season. This is in agreement with previous results by Gacic et al. (1997) based on the analysis of SST data, which show a major Ionian water inflow during fall, reaching the northern basin along the eastern coast. The Gacic et al. (1997) results also suggest that during spring and summer the circulation is probably too weak and fragmented to support a consistent northern current.

As for the dynamical reason behind the enhanced fall exchange, different possible mechanisms can be envisioned: a

thermohaline one, by which the first storms in the northern part determine an enhanced evaporation, which in turn increases the flux of entering water; a mechanical mechanism, related to the presence of southerly winds over the basin or of an atmospheric pressure gradient during the late summer–fall months ([Maggiore et al. 1998](#); [Kovacevic et al. 1999](#)).

#### *a. Exchange between deep and coastal regions in the southern basin*

As mentioned in [section 2c](#), the mean field ([Fig. 1c](#)) obtained by the pseudo-Eulerian analysis of the drifter data suggests a strong influence of the bottom topography on the surface flow pattern. This aspect is particularly important for a basin with coastal characteristics like the Adriatic Sea. Therefore, we focused our analysis on the influence of topography on the trajectories and on the fluid exchange at the surface between coastal and offshore regions.

We first reconstructed the bottom topography corresponding to the drifter trajectories; this was done attributing to each drifter location the corresponding bottom depth obtained from the interpolation of a bathymetric dataset with a resolution of 1/30 degree ([Smith et al. 1997](#); the dataset is available on the World Wide Web via [ftp://topex.ucsd.edu/pub/global\\_topo\\_2min](ftp://topex.ucsd.edu/pub/global_topo_2min)). The analysis was carried out in detail for the southern Adriatic where more data are available. As shown in [Fig. 1b](#), most of the drifters deployed in the Strait of Otranto appear to span the whole area. This is mirrored by the distribution of the bottom depths corresponding to the drifter trajectories: [Fig. 3a](#) shows the depth distribution, which would seemingly suggest a preponderance of relatively shallow trajectories ( $z < 200$  m). The Adriatic Sea, however, even in its southern subarea, is a relatively shallow basin, and the predominance of shallow trajectories is just a consequence of the uneven distribution of the bottom depths. [Figure 3b](#) shows the same data weighted with the geographical extent of the region characterized by the bottom depths corresponding to each class; in other words, it reports the data presented in [Fig. 3a](#) normalized, class by class, by the corresponding distribution of the bottom depths in the southern Adriatic. The resulting distribution is much flatter than the one shown in [Fig. 3a](#). This suggests that the drifters do not sample any preferential range of depths, with a possible exception for the depths  $< 100$  m. Bottom topography thus does not seem to have a strong role as a dynamical constraint, and the probability of finding a particle at a specific position is not heavily affected by the corresponding bottom depth.

The possibility of fluid exchange at the surface among regions characterized by different bottom depths is witnessed by a comparison between [Figs. 3b and 3c](#); the latter shows the distribution of the (nonnormalized) bottom depth corresponding to the trajectory entrance point into the southern Adriatic, crossing  $40.4^\circ\text{N}$ . The comparison between [Fig. 3b](#) and the “initial conditions” ([Fig. 3c](#)) shows that the “initial” bottom depths span the range 0–900 m (the maximum depth reached in the Strait of Otranto is over 800 m), whereas the drifter trajectories in their successive development will invade regions characterized by much deeper topography, confirming the existence of fluid exchange mechanisms that are not constrained by a Lagrangian conservation of the corresponding bottom depths. This is not surprising since drifters are in the upper meter of the water column and are therefore subject to transient wind forcing and to stratification effects, which, as discussed above, might isolate the flow from the influence of bottom topography. That the drifters are not perfectly Lagrangian (relative slip of  $2\text{--}3\text{ cm s}^{-1}$  with respect to the real currents; [Poulain 1999](#)) can also increase the cross-isobath drifter crossings. As a consequence, the real transports might be slightly overestimated. This problem will have to be taken into account if one wants to give quantitative estimates of cross-topography transports using drifter data.

#### **4. A transport model applied to the Lagrangian data**

An important outcome of the analysis of Lagrangian data is the computation of transport parameters that can be used in simple transport models such as the advection–diffusion equation (e.g., [Davis 1987, 1991](#); [Griffa et al. 1995](#)). The use of these models is very appealing because they allow statistical prediction of tracer transport using only some reduced statistical information on the velocity field. Conceptually, these models assume that the velocity field has two distinct components: a large-scale mean flow  $U$  and a turbulent mesoscale field  $u'$ . Correspondingly, the tracer particles are advected through two separate processes, the advection by  $U$  and the turbulent transport due to  $u'$ , which is characterized by some simple transport parameters such as the eddy diffusivity  $K$  ([Taylor 1921](#)). In principle,  $K$  is an observable, and Lagrangian data are especially suitable to estimate it because they provide direct transport measurements (e.g., [Colin de Verdiere 1983](#); [Swenson and Niiler 1996](#)).

Despite the appeal of this conceptual simplicity, the application of models of this type to ocean flows can be sometimes problematic because the flow decomposition in mean and eddy field may be not well defined, especially when the large-scale flow is highly inhomogeneous and nonstationary. Problems arise, for instance, when there is no clear spectral gap between mean flow and eddy velocity (e.g., [Holloway 1989](#); [Zambianchi and Griffa 1994](#)), or when the data are not sufficient to properly resolve the time- and space scales of the flow.

In the case of the Adriatic Sea,  $U$  is nonstationary at seasonal and longer scales, and the eddy statistics are inhomogeneous over the basin. The available dataset, on the other hand, does not allow one to resolve the time and space variations. As discussed in [section 2](#) and in the following,  $U$  can be estimated only as an ensemble average over the whole period of measurements, and the turbulent parameters can be computed only as constants over the whole basin. We know

then that the flow decomposition will be imperfect. The question is to what extent and, in particular, whether or not it can be effectively used as a basis for a transport model.

In the following, these points are first tested by performing an optimized flow decomposition that provides values for  $U$  and for the transport parameters, and then by using them in a simple transport model. The decomposition was carried out using the entire dataset of 41 drifters.

The model is Lagrangian in nature. Hence it is especially suitable for the comparison with Lagrangian data. The consistency of the decomposition and the performance of the model are checked a posteriori by comparing the model outputs with results from a subset of the data, consisting of the 31 drifters entering the basin through the Strait of Otranto. Thus, the comparison involves the statistics of particle spreading from a pointlike source. The details of the model, decomposition, and tests are described below.

### a. Description of the model

The model used is Lagrangian; that is, it simulates the motion of independent particles in a turbulent flow. It can be used to study dispersion of passive tracers by simulating a high number of particles that can be considered as tracer particles. Their concentration corresponds to the average concentration of the tracer itself ([Csanady 1989](#)).

The model belongs to the general class of “random flight” models (e.g., [Thomson 1987](#)) and is commonly used in atmospheric and oceanic physics (e.g., [Thomson 1986](#); [Dutkiewicz et al. 1993](#)). In the case of homogeneous turbulence in two dimensions (representing the ocean surface), the model for each component can be written in incremental form as

$$dx = (U + u') dt \quad (1)$$

$$du' = -(1/T_L)u' dt + \sqrt{(\sigma^2/T_L)} dw, \quad (2)$$

where  $\sigma^2$  is the variance,  $T_L$  is the turbulence decorrelation timescale, and  $dw$  is a random increment from a normal distribution with zero mean and second-order moment  $\langle dw(t_i) dw(t_j) \rangle = \delta_{ij} 2dt$ . Here  $T_L$  is defined as

$$T_L = \frac{1}{\sigma^2} \int_0^\infty dt \langle du'(0) du'(t) \rangle. \quad (3)$$

Conceptually, (2) states that the turbulent velocity  $u'$  following particles is a linear Gaussian–Markov process, characterized by an exponential autocovariance with  $e$ -folding timescale  $T_L$  ([Risken 1989](#)). This is, of course, a crude model of real turbulence, but it is supported by experimental and numerical results in fully developed turbulence ([Yeung and Pope 1989](#)) and it also appears appropriate for mesoscale oceanic flows, at least at the surface (e.g., [Krauss and Böning 1987](#); [Colin de Verdiere 1983](#); [Griffa 1996](#)).

It can be shown (e.g., [Risken 1989](#); [Zambianchi and Griffa 1994](#)) that, with respect to the advection–diffusion equation, the model (1)–(2) has a broader range of applicability because it is not as strictly based on the assumption of scale separation between mean flow and turbulent eddy field. On the other hand, when the scale separation holds, (1)–(2) is equivalent to the advection–diffusion equation for  $t \gg T_L$ , and the two parameters  $\sigma^2$  and  $T_L$  are related to the diffusivity parameter  $K$  in the advection–diffusion equation by the relationship

$$K = \sigma^2 T_L. \quad (4)$$

For practical applications, model (1)–(2) needs the values of the mean field  $U$  and of the turbulent parameters  $\sigma^2$  and  $T_L$  as input parameters. These values are computed from the data, performing a flow decomposition as shown in the following.

### b. Flow decomposition

Often, in the oceanographic literature (e.g., [Swenson and Niiler 1996](#); [Poulain 1999](#)), the flow decomposition in mean flow and eddy field is performed doing first a partition of the geographical domain into bins, as shown in [section 2](#). The flow inside each bin is assumed to be homogeneous and stationary, and the mean flow is computed as the average of all the velocity measurements available in the bin. The departure from the constant mean is interpreted as representative of the eddy

field inside the bin and is represented by statistical quantities such as  $\sigma^2$ ,  $T_L$ , or  $K$ . Notice that in this context the word “eddy” is used loosely to indicate all the fluctuations occurring at synoptic scales, including actual eddies due to instabilities as well as wave phenomena, wind-driven current reversals, and possible long-term variability at seasonal and interannual scales.

Problems can arise when the mean flow is highly inhomogeneous in the region of interest, so the bins have to be small enough to appropriately resolve the inhomogeneity. Often, in these cases, the resulting bins are too small to allow for sufficient data density (i.e., the drifters do not spend enough time in a bin) to estimate significantly  $T_L$  or  $K$  using the nonlocal, asymptotic estimates (3)–(4). This is the case in the Adriatic Sea, where the inhomogeneity of the large-scale currents requires a binning of at least  $0.25^\circ \times 0.25^\circ$  as discussed in [section 2](#). This bin size is not sufficient to significantly estimate  $T_L$  or  $K$ .

An alternative method to perform the flow decomposition has been recently developed by [Bauer et al. \(1998\)](#). This method relaxes the requirement of homogeneity by requiring that only the eddy field is approximately homogeneous inside bins, while the large-scale mean flow can be space dependent and characterized by shear. The method consists in estimating  $U$  using a bicubic spline interpolation whose parameters are optimized to minimize the energy in the fluctuation field at low frequency. Since the considered “bins” only require homogeneity in the eddy field, their size is usually larger, so that the estimates of  $T_L$  and  $K$  are in general more reliable because they are based on more data and longer trajectories.

This is the method that we used for the Adriatic Sea. In theory, the method should be applied to subsets of data that are approximately stationary, for example, corresponding to a specific season, and inside subregions where the eddy statistics is homogeneous, identified, for example, by constant kinetic energy regions. In reality, the data density is too scarce for such a partition, and we are forced, in order to have reliable estimates, to use the whole dataset. Some a posteriori checks have been performed, dividing the basin in two subregions and considering separately the winter and summer seasons. The results are not significantly different at the precision allowed by the dataset. Details on the application of the method and on the a posteriori checks are shown in appendixes A and B, respectively. Here we discuss only the main results.

In [Fig. 4](#) we show the estimate for the large-scale mean flow  $U$  ([Fig. 4a](#)), together with the autocovariances and diffusivities  $K$  ( $K_u$ ,  $K_v$ ) of the fluctuations ([Fig. 4b](#)). The  $U$  estimate is obviously similar, qualitatively and quantitatively, to the one obtained using the  $0.25^\circ \times 0.25^\circ$  binning in [Fig. 2b](#). The autocovariances and diffusivities show some anisotropy, with the meridional component being more energetic. This is probably related to the strong north–south wind-induced fluctuations along the Albanian coast. Also, it can be seen that the autocovariances (especially the meridional one) do not completely vanish for  $t > 10$  days, and correspondingly  $K_v$  does not converge exactly to a constant. This is likely to be a consequence of the large-scale residuals. On the other hand, it should be noted that the statistics are relatively close to convergence, suggesting that the decomposition might be acceptable, despite the lack of complete resolution of time and space scales. Moreover, since the Adriatic is a closed, relatively small basin, the diffusion coefficient is going to vanish asymptotically since after a certain time the particle will have spread over the whole basin and their residual square distance will not be able to increase indefinitely. This is an intrinsic weakness of the use of an asymptotic quantity such as the diffusivity for the study of dispersion in a finite size basin, which may be solved by the use of more appropriate descriptions (e.g., the finite size Lyapunov exponents: see [Artale et al. 1997](#); [Lacorata et al. 2000](#)). However, since we are interested in timescales of the order of several tens of days, up to 100 or 200 days at the most, we estimate  $K$  when the corresponding curve shows that sort of intermediate saturation regime evident in [Fig. 4b](#).

From [Fig. 4b](#), some simple quantitative estimates of the parameters  $\sigma^2$  ( $\sigma_u^2$ ,  $\sigma_v^2$ ),  $K$  ( $K_u$ ,  $K_v$ ), and  $T_L$  ( $T_{Lu}$ ,  $T_{Lv}$ ) can be computed for each component. The variance appears to be approximately  $\sigma_u^2 = 80 \text{ cm}^2 \text{ s}^{-2}$  and  $\sigma_v^2 = 110 \text{ cm}^2 \text{ s}^{-2}$  for the meridional and zonal components, respectively. The diffusivity is  $K_u \approx 1 \times 10^7 \text{ cm}^2 \text{ s}^{-1}$  for the meridional component and  $K_v \approx 3 \times 10^7 \text{ cm}^2 \text{ s}^{-1}$  for the zonal component. The values of  $T_L$  for the two components can be estimated using (4), suggesting  $T_{Lu} \approx 1.4$  days and  $T_{Lv} \approx 3$  days for the meridional and zonal components, respectively.

A histogram of the values of the fluctuating field  $u'$  is shown in [Fig. 5](#). The histogram provides an estimate of the probability density function (pdf) of the fluctuating velocity. As it can be seen, the pdf shows a clear deviation from Gaussian, especially in the tails. Deviations from gaussianity have been observed in other oceanographic flows ([Swenson and Niiler 1996](#); [Bracco et al. 2000](#)), especially in the case of highly nonlinear flows. Here the deviation is likely to be enhanced by the presence of inhomogeneity and nonstationarity in the eddy field. Quantitatively, the deviation is mainly evident in the highest 10% values of the velocity. In the model (1)–(2) the distribution of  $u'$  is assumed Gaussian. Deviations from Gaussianity are expected to affect mainly statistics involving moments of order higher than 2 (e.g., [Bracco et al. 2000](#)).

### c. Model implementation

The transport model (1)–(2) was implemented using the estimate of  $U$  obtained by the above bicubic spline interpolation method (Fig. 4) with a resolution of 10 km, and values of  $\sigma^2$  and  $T_L$  in the range suggested by the data:  $\sigma^2_{u(\mathbf{U})} = 80$  (110)  $\text{cm}^2 \text{s}^{-2}$  and  $T_L = 1.5$  (2.7) days for the zonal (meridional) component. The time step is  $dt = 30$  min, chosen after a number of preliminary tests (Buffoni et al. 1997). Because of the low data density in the northern part of the basin, the  $U$  field is set to zero north of  $44.7^\circ\text{N}$ . Each particle trajectory is obtained integrating (1)–(2) with a different realization of the turbulent process and interpolating  $U$  between grid points using a fourth-order Lagrangian interpolation scheme (Hua 1994).

Reflection boundary conditions are used at the closed boundaries, which represent the simplest way to guarantee the well-mixed condition (Thomson 1987). At the southern boundary, where the basin is open and communicates with the rest of the Mediterranean Sea, particles are free to enter and exit following the current, characterized by inflowing motion at the eastern side and outflowing motion at the western side. When particles leave the basin (moving south of  $40.4^\circ\text{N}$ ), following the outflow, they are considered lost and cannot reenter. This condition has been used in a number of previous works (Buffoni et al. 1997) and models a physical situation where there is a strong advective current exiting the basin so that the particles are flushed away and do not reenter.

In the case of the Adriatic Sea, the drifter data suggest that this “advective” boundary condition is indeed appropriate for most of the drifters since they exit the basin following the strong boundary current close to the western coast and do not reenter the basin. There is a small subset of  $n_S = 3$  drifters, however, that, soon after the release, become trapped in eddies localized at the basin entrance and are entrained in the outflow current (see, e.g., Fig. 3a). These drifters exit the basin (i.e., they move south of  $40.4^\circ\text{N}$ ) after a few days ( $<15$  days) and then recirculate in the Strait of Otranto, eventually reentering the basin. Therefore, they are not well represented by the advective boundary condition. This point will be considered and accounted for when the model results are compared with the data.

### d. Model evaluation

The model is tested against the data, verifying whether or not it is able to reproduce the statistics of a given subset of particles. Conceptually, this addresses the question of existence of a set of parameters,  $U$ ,  $\sigma^2$ , and  $T_L$ , such that the model (1)–(2) can reproduce reality. Similar conceptual questions have been previously addressed, for example, in the framework of numerical models by Figueroa and Olson (1994), who studied whether or not an advection–diffusion equation with parameters computed from (synthetic) Lagrangian data can reproduce tracer transport in an idealized double gyre.

In the following, we will test the model using the subset of 31 particles entering the basin through the Strait of Otranto (Table 1), that is, approximately characterized by a point release. Their statistics will be compared with the statistics of simulated particles deployed on the eastern side of the strait at a latitude of  $40.4^\circ\text{N}$ .

In order to perform the comparisons significantly, two systematic differences between real and simulated trajectories have to be taken into account. The first difference is that real drifters stop transmitting useful data after a time on the order of  $\approx 100$  days, with a maximum lifetime of 220 days. The particles simulated by (1)–(2), however, do not have such a limit except for their exit from the basin. This difference was eliminated by imposing a limited lifetime on simulated drifters. The lifetime of each of them is a random value from a “mortality” distribution shaped so as to resemble one of the real drifters. Details on this distribution are discussed later.

The second difference is that, as mentioned above, a subset of  $n_S$  real drifters recirculates at initial time in and out of the basin, while particles simulated with the boundary conditions illustrated in section 4c cannot reproduce this behavior. To account for this difference in the comparison, we truncate the real drifters when they exit the basin passing through the  $40.4^\circ\text{N}$  boundary. If they reenter after a time longer than 15 days (more than five times  $T_L$ ), they are recounted as new independent particles. This happens for two drifters, so the set of particles for the comparison is 33 instead of the original 31.

Regarding the simulations, 10 realizations of 33 particles each are considered so that a statistical range of results can be established. The goal is to verify whether or not the real data can be statistically considered as one realization of the model. A number of comparison tests are performed on the ensemble statistics without considering seasonality. They thus characterize the most likely behavior of the particles during the whole measurement period.

## 1) QUALITATIVE COMPARISON OF TRAJECTORIES

As a first test, a qualitative comparison between the real and simulated particle behavior is carried out. It is found that



simulated trajectories have characteristics very similar to the real ones, exhibiting all the different types of behavior discussed in [section 3](#) (trapping in the southern region, recirculation in the central basin, extension to the northern basin). Examples showing the qualitative similarity of simulated and real trajectories are shown in [Fig. 6](#).

## 2) COMPARISON OF STATISTICAL PROPERTIES

A more quantitative comparison is done considering some statistical properties of the ensemble. More specifically, we have computed, for each set of 33 simulated particles,

1. the number  $n_S$  of particles that exit the basin after a short time ( $t < 15$  days) from release;
2. the number  $n_N$  of particles that get to the northern basin;
3. the total number  $n_T$  of particles that exit the basin; and
4. the mean value,  $\hat{T}_1$ , of the (first) exit time of the  $n_T$  particles leaving the basin.

The results, summarized in [Table 2](#), show good agreement between real and simulated particles.

The robustness of these results has been tested by performing a number of sensitivity tests. First of all, we have considered the shape of the mortality distribution, modeled after that of the real drifters. We have kept fixed the maximum value of the drifter lifetime (220 days) and have varied the details of the distribution. The results in [Table 2](#) have been obtained for a flat distribution between 10 and 220 days. We have also used a flat distribution between 50 and 220 days and a distribution with a maximum between 100 and 150 days. The values of the statistics reported in [Table 2](#) do not vary significantly (less than 5%), showing that the details of the distribution are not important.

We have then tested the dependence of the results on the turbulent transport parameters  $\sigma^2$  and  $T_L$  by varying them within a factor of 3. The results show a quite strong sensitivity on the flow decomposition and confirm that the values derived by the analysis described in [section 4b](#) are indeed appropriate.

Finally, we have tested the sensitivity of the data statistics with respect to the specific definition for the entrance of the Adriatic basin using a boundary at  $40.2^\circ\text{N}$  instead of  $40.4^\circ\text{N}$ . The results show that there is some dependence on the specific definition of the basin but the simulation results are acceptable for a reasonable range of latitudes north of  $40^\circ\text{N}$  in the Strait of Otranto. The dependence become stronger south of  $40^\circ\text{N}$ , where the effects of the boundary with the Ionian Sea become more evident and an increasing number of particles tend to exit quickly from the Adriatic Sea, entering the Ionian and staying there.

## 3) COMPARISON OF PARTICLE DISPERSION

As a last test, we have considered the space and time evolution of the dispersion of particles released at the Strait of Otranto. We have simulated 1000 particles starting from initial conditions along the eastern part of the  $40.4^\circ\text{N}$  section. We have studied the diffusive clouds for the following 200 days, verifying whether or not the real drifter positions find themselves within the cloud. If so, this is an indication that the dispersion simulated by the model can explain the ensemble average dispersion of the data over the measurement period.

The results are shown in [Fig. 7](#). In the first 10 and 20 days, the simulated particles appear to be advected northward, while spreading under the effect of enhanced shear dispersion. Starting from  $t \approx 30$  days, the particles tend to spread over the whole longitudinal length of the southern basin due to the combined effect of diffusion and advection by the southward return currents. By  $t \approx 100$  days, the particle concentration  $c(t, \mathbf{x})$  is approximately homogeneous over the southern, central, and part of the northern regions of the basin. The concentration progressively decreases as particles leave the basin from the outflow. The homogenization and progressive decrease of  $c(x, t)$  is characteristic of semienclosed basins with recirculations ([Buffoni et al. 1997](#)).

The drifter data are superimposed onto the simulated particles in [Fig. 8](#). They show a pattern analogous to the simulation, falling at almost all times inside the modeled dispersive cloud. The only exceptions are found at an intermediate time, between 20 and 40 days, when a subset of four drifters overcome the cloud, being advected very quickly to the north and recirculating to the south. All four drifters belong to the late summer release, suggesting an especially strong event. Note that these drifters, characterized by a swift northward velocity, are responsible for the high positive values in the tail of the velocity probability density function in [Fig. 5](#).

In summary, the model appears to capture successfully the dispersion behavior of the real particles, except for an intermediate time interval during the advective event in late summer.

## 5. Estimates of residence time

In many situations, when the interest is focused on the basin-scale properties of dispersion rather than on the details of the mixing process, it is useful to characterize the macroscopic dispersion behavior in a basin using suitable integral quantities (e.g., [Taylor 1953](#)). For example, the spreading of a substance initially released in a semi-enclosed basin can be described considering the time evolution of its total (normalized) amount in the basin,  $C(t)$ , and its residence time,  $T$ , defined as ([Buffoni et al. 1997](#))

$$C(t) = \int_{\Omega} c(t, \mathbf{x}) d\mathbf{x}, \quad (5)$$

$$T = \int_0^{\infty} C(t') dt', \quad (6)$$

where  $c(t, \mathbf{x})$  is the average normalized tracer concentration at point  $\mathbf{x}$  and time  $t$ , and  $\Omega$  represents the basin. Here  $T$  is a measure of the average time spent by a tracer particle in the basin and is a useful indicator for biological and chemical processes, as well as for water mass mixing.

[Buffoni et al. \(1997\)](#) have defined  $C(t)$  and  $T$  in the Lagrangian framework as

$$C(t) = N(t)/N(0) \quad (7)$$

$$T = \lim_{t \rightarrow \infty} T^*, \quad (8)$$

$$T^* = tN(t)/N(0) + \sum_{i=1}^{N_e(t)} t_{ei}/N(0), \quad (9)$$


where  $N(0)$  is the number of tracer particles initially deployed in the basin,  $N(t)$  is the number of particles at time  $t$ ,  $N_e$  is the number of particles that have already escaped the basin at time  $t$ ,  $t_{ei}$  is the escape time of the  $i$ th particle, and the particles are ordered as a function of their escape time (particle 1 is the first one to escape). Then  $T$  corresponds to the average first exit time computed over a very high number of particles.

Here we use the drifter data released at the Strait of Otranto to obtain information on  $T$ . In principle, [expressions \(8\)–\(9\)](#) could be used directly to provide an estimate  $\hat{T}$  from the data. In practice, though, there are some specific issues that have to be taken into account.

First of all, the dataset that we use is very small since only 13 drifters of the original 33 exit from the basin (see [Table 2](#)) and can be used in [\(9\)](#). As a consequence, the estimate is expected to have a significant variance error. Also, the drifters have a finite lifetime, and this is expected to produce a significant bias error. Only particles with exit times  $t_{ei} < 220$  days are used in the asymptotic estimate [\(8\)–\(9\)](#), while the others, which terminate inside the basin, cannot be used. The bias is therefore expected to be toward fast exiting particles and short values of  $T$ . This point will be addressed specifically in [Section 5a](#), using results from the transport model [\(1\)–\(2\)](#).


The second issue to consider is that the definition of the exit time  $t_{ei}$  in [\(9\)](#) is not straightforward for the  $n_S$  particles that recirculate and reenter the basin. The question is when exactly they have to be considered “inside” or “outside” the basin. In other words, one can imagine the existence of a “buffer” zone at the southern end of the basin such that particles inside the buffer can still be considered inside the basin. The difficulty lies in the definition of the buffer zone, which is conceptually arbitrary.



In the following, in order to identify a range of possible values for the estimate  $\hat{T}$ , we consider two extreme choices for the buffer zone.

1. Zero buffer zone. In this case particles that exit from the basin are immediately considered outside and not allowed to reenter. This is the same choice used in [section 4](#) and corresponds to truncate the drifters when they move south of  $40.4^\circ\text{N}$ . In this case, the estimate of  $T$  corresponds exactly to the  $\hat{T}_1$  computed in [section 4](#) ([Table 2](#) ). Its value is  $\hat{T}_1 = 69$  days.
2. Maximum buffer zone. In this case the buffer is chosen to contain all the recirculating drifters, which are therefore considered inside during their whole life. This corresponds to choosing a region between  $40.4^\circ$  and  $39.4^\circ\text{N}$ , just south of the Strait of Otranto at the border with the Ionian Sea. In this case the estimate of  $T$  is  $\hat{T}_2 = 88$  days.

### a. Error estimates

We first consider choice 1, which is exactly reproducible using model (1)–(2) with the advective boundary condition discussed in [section 4](#). The errors are estimated first performing simulations with a high number (1000) of particles released at the entrance of the basin, to obtain the “true”  $T$  value, that is, computed without limitations in particle number and lifetime. Then, as done in [section 4](#), we consider 10 realizations with 33 particles each and with a mortality function to investigate the associated errors.

The results for the true  $C$  and  $T^*(t)$  from (7)–(9) are shown in [Fig. 8](#) . Here  $C(t)$  initially decreases abruptly because of the  $n_S$  particles initially caught in eddies and entrained in the outflow. Then, after  $\sim 15$ – $20$  days the decay rate decreases, and for  $t > 50$  days it becomes approximately exponential. Fifty days corresponds to an estimate of the advection time, that is, the time for a particle to go around the southern basin, and the exponential decay for  $C(t)$  is expected to occur in a semienclosed basin, after the initial advective phase ([Buffoni et al. 1997](#)). The asymptotic values of  $T^*(t)$  show a convergence to  $T \simeq 190$  days, which is significantly higher than the estimate from the data.

The behavior of the estimates of  $C(t)$  and  $T^*$  for the 10 realizations of particles with mortality is also shown in [Fig. 8](#) . All the estimates  $\hat{T}$  are consistently lower than the true  $T$  with an average value of 61 days (see also [Table 2](#) ) , which suggests a bias of approximately 67% due to the finite lifetime. The rms error around the mean value, due to the finite sampling, is approximately 20%.

The results obtained from the drifters (thick curves) are superimposed on the results of the simulations. As already noticed in [section 4](#), they fall in the envelope of the simulations, suggesting that the numerical results are representative of the situation sampled by the real drifters.

Regarding choice 2, obtaining a numerical analog of it is not straightforward because the choice of the appropriate southern boundary conditions for particle motion is not obvious. We expect, though, that the results will be different from those of choice 1 mainly at initial times. In particular,  $C(t)$  will not decrease as sharply for  $t < 15$ – $20$  days since the  $n_S$  particles are not considered as outside. The behavior at longer times is expected to be similar. Since  $T$  is the asymptotic integral of  $C(t)$  [see (6)], its value for choice 2 is expected to be at least as high as the one obtained with choice 1. As a consequence, the value for choice 1 can be considered as a lower limit of  $T$ .

In summary, direct estimates of  $T$  from the drifters provide values of the order of 70–90 days. The numerical results suggest a high bias error (up to 65% and more) due to fact that drifters have a finite lifetime and place the true value of  $T$  around 200 days.

It is worth adding that the residence time  $T$  is, by definition, a quantity that depends on the position of the particle release. We can expect this to be especially true when the release is near the boundary of the basin. As suggested in [section 4d](#), the previous results are likely to hold for releases north of  $40^\circ\text{N}$ , while releases south of  $40^\circ\text{N}$  are expected to behave differently since they would be directly influenced by the circulation at the northern boundary of the Ionian Sea.

## 6. Discussion and conclusions

The trajectories described by 41 drifters between December 1994 and March 1996 were used to study the surface transport properties in the Adriatic Sea. Due to the finite lifetime of the drifters, the information gained from the Lagrangian data is representative of transport over the first 100 days after deployment. As a consequence, some of the statistics calculated from the drifter data are biased. For example, the basin residence timescale is significantly underestimated.

First, we characterized the transport of passive tracers entering the Adriatic Sea through the Strait of Otranto. Three main different types of trajectories were observed: 1) some of the drifters recirculated directly in the Strait of Otranto, 2) others

recirculated in the southern and central subbasins during one or two months, and finally 3) some of them reached the northern basin. The exchange between the southern and northern basins appeared to be maximum in late summer and early fall. The dynamical reason behind the increased exchange can be speculated in terms of thermohaline (enhanced evaporation that increases the flux of entering water) and mechanical (southerly winds, along-basin pressure gradient) forcings.

Second, the exchange properties between deep sea and shallow coastal shelf regions were investigated by following the drifters deployed in the Strait of Otranto. Despite the obvious topographic steering of the mean circulation (as seen in the mean flow maps of [Figs. 1c](#) and [4a](#)) our analyses disclose that there is significant cross-topography or cross-shelf exchange. This is mostly due to the turbulent component of the velocity field. However, the persistence of a tendency to cross isobaths even after filtering out the turbulent and transient components of the velocity field leads us to hypothesize a relevant role of the stratification in the definition of the lower limit of the surface layer; this cross-isobath mixing is more strongly felt in open sea areas whose depth is greater than  $\approx 100$  m.

Third, a simple Lagrangian model with parameters derived from the drifter data was developed. The flow decomposition in mean flow and eddy field was done using the method described in [Bauer et al. \(1998\)](#) by minimizing the energy of the fluctuating field at low frequency. The eddy field derived by the spline method and utilized in the Lagrangian model results larger in the meridional direction, probably due to the north–south orientation of the Strait of Otranto and of the Albanian coast, where strong wind-induced fluctuations occur and where the observation density is especially high. The model simulations were compared with drifter data released in the Strait of Otranto considering 1) the qualitative behavior of the trajectories, 2) the main statistical properties of the ensemble, and 3) the patterns of particle dispersion. The agreement between data and model results is very satisfactory except for an intermediate interval during a strong advective event that occurred in late summer. During this event, the velocity of the real drifters significantly exceeds the velocity of the simulated particles. Aside from this event, the model appears able to reproduce reality with good approximation.

Finally, an important characteristic parameter of the Adriatic surface transport, the residence timescale in the basin, was estimated from the drifter observations and from the model simulations. This parameter provides an answer to the following question: How long does a particle entering the Adriatic through the Strait of Otranto (near 40°N) take before exiting the basin, supposing that the particle stays at the surface at all times? Vertical velocities and sinking of surface water during events of deep-water formation are thus ignored. The estimate obtained from the drifter data is between 70 and 90 days, whereas the model suggests a residence timescale around 200 days. This difference is expected given the limited lifetime of the drifters. One of the main successes of our advection–diffusion model, tuned with drifter-inferred parameters, is its ability to estimate a realistic, unbiased residence time for the surface Adriatic basin.

### Acknowledgments

The authors wish to thank Sonia Bauer, who kindly provided the code for the flow decomposition utilizing the bicubic spline technique. Thanks also to Alessio Bellucci, who did some preliminary work on the Lagrangian measurements, and to Donatella Faggioli, who helped retrieve the bathymetric data. Support from the Office of Naval Research under Contracts N00014-97-1-0620 (A. Griffa) and N0001499WR30014 (P.-M. Poulain), from the European Social Fund (objective 1), from the Italian Ministry of Scientific and Technological Research, and from the Italian National Research Council is gratefully acknowledged.

---

### REFERENCES

Artale, V., G. Boffetta, A. Celani, M. Cencini, and A. Vulpiani, 1997: Dispersion of passive tracers in closed basins: Beyond the diffusion coefficient. *Phys. Fluids*, **9**, 3162..

Artegiani, A., D. Bregant, E. Paschini, N. Pinardi, F. Raicich, and A. Russo, 1997a: The Adriatic Sea general circulation. Part I: Air–sea interactions and water mass structure. *J. Phys. Oceanogr.*, **27**, 1492–1514.. [Find this article online](#)

—, —, —, —, —, and —, 1997b: The Adriatic Sea general circulation. Part II: Baroclinic circulation structure. *J. Phys. Oceanogr.*, **27**, 1515–1532.. [Find this article online](#)

Bauer, S., M. S. Swenson, A. Griffa, A. J. Mariano, and K. Owens, 1998: Eddy-mean flow decomposition and eddy-diffusivity estimates in the tropical Pacific Ocean. Part 1: Methodology. *J. Geophys. Res.*, **103** (C13), 30 855–30 871..

Bergamasco, A., and M. Gacic, 1996: Baroclinic response of the Adriatic Sea to an episode of bora wind. *J. Phys. Oceanogr.*, **26**, 1354–1369.. [Find this article online](#)

Bracco, A., J. LaCasce, and A. Provenzale, 2000: Velocity probability density functions for oceanic floats. *J. Phys. Oceanogr.*, **30**, 461–474.. [Find this article online](#)

- Buffoni, G., P. Falco, A. Griffa, and E. Zambianchi, 1997: Dispersion processes and residence times in a semi-enclosed basin with recirculating gyres. An application to the Tyrrhenian Sea. *J. Geophys. Res.*, **102** (C8), 18 699–18 713..
- Buljan, M., and M. Zore-Armanda, 1976: Oceanographical properties of the Adriatic Sea. *Oceanogr. Mar. Biol. Ann. Rev.*, **14**, 11–98..
- Colin de Verdiere, A., 1983: Lagrangian eddy statistics from surface drifters in the eastern North Atlantic. *J. Mar. Res.*, **41**, 375–398..
- Csanady, G. T., 1989: *Turbulent Diffusion in the Environment*. D. Reidel, 248 pp..
- Davis, R. E., 1985: Drifter observations of coastal currents during CODE. The method and descriptive view. *J. Geophys. Res.*, **90**, 4741–4755..
- , 1987: Modeling eddy transport of passive tracers. *J. Mar. Res.*, **45**, 635–666..
- , 1991: Observing the general circulation with floats. *Deep-Sea Res.*, **38** (Suppl. 1), S531–S571..
- Dutkiewicz, S., A. Griffa, and D. Olson, 1993: Particle diffusion in a meandering jet. *J. Geophys. Res.*, **98** (C9), 16 487–16 500..
- Figueroa, H. A., and B. Olson, 1994: Eddy resolution versus eddy diffusion in a double gyre GCM: The Lagrangian and Eulerian description. *J. Phys. Oceanogr.*, **24**, 371–386.. [Find this article online](#)
- Gacic, M., S. Marullo, R. Santoleri, and A. Bergamasco, 1997: Analysis of seasonal and interannual variability of the sea surface temperature field in the Adriatic Sea from AVHRR data (1984–1992). *J. Geophys. Res.*, **102** (C10), 22 937–22 946..
- , G. Civitarese, and L. Ursella, 1999: Spatial and seasonal variability of water and biogeochemical fluxes in the Adriatic Sea. *The Eastern Mediterranean as a Laboratory Basin for the Assessment of Contrasting Ecosystems*, P. Malanotte-Rizzoli and V. N. Eremeev, Eds., Kluwer Academic, 335–357..
- Griffa, A., 1996: Applications of stochastic particle models to oceanographic problems. *Stochastic Modelling in Physical Oceanography*, R. J. Adler, P. Muller, and B. L. Rozovskii, Eds., Birkhauser, 114–140..
- , K. Owens, L. Piterbarg, and B. Rozovskii, 1995: Estimates of turbulence parameters from Lagrangian data using a stochastic particle model. *J. Mar. Res.*, **53**, 371–401..
- Grilli, F., and N. Pinardi, 1998: The computation of Rossby radii of deformation for the Mediterranean Sea. *MTP News*, **6**, 4..
- Hansen, D. V., and P.-M. Poulain, 1996: Processing of WOCE/TOGA drifter data. *J. Atmos. Oceanic Technol.*, **13**, 900–909..
- Holloway, G., 1989: Subgrid scale representation. *Oceanic Circulation Models; Combining Data and Dynamics*, L. T. Anderson and J. Willebrandt, Eds., NATO ASI Series, 513–587..
- Hua, B. L., 1994: The conservation of potential vorticity along Lagrangian trajectories in simulations of eddy-driven flows. *J. Phys. Oceanogr.*, **24**, 498–508.. [Find this article online](#)
- Inoue, H., 1986: A least square smooth fitting for irregularly spaced data: Finite element approach using the cubic  $\beta$ -spline. *Geophysics*, **51**, 2051–2066..
- Kovacevic, V., M. Gacic, and P.-M. Poulain, 1999: Eulerian current measurement in the Strait of Otranto and in the southern Adriatic. *J. Mar. Syst.*, **20**, 255–278..
- Krauss, W., and C. Boning, 1987: Lagrangian properties of eddy fields in the northern North Atlantic as deduced from satellite-tracked buoys. *J. Mar. Res.*, **45**, 259–291..
- Lacorata, G., E. Aurell, and A. Vulpiani, 1999: Data analysis and modelling of Lagrangian drifters in the Adriatic Sea. *J. Mar. Res.*, in press..
- Maggiore, A., M. Zavatarelli, M. G. Angelucci, and N. Pinardi, 1998: Surface heat and water fluxes in the Adriatic Sea: Seasonal and interannual variability. *Phys. Chem. Earth*, **23**, 561–567..
- Malanotte-Rizzoli, P., and A. Bergamasco, 1983: The dynamics of the coastal region of the northern Adriatic Sea. *J. Phys. Oceanogr.*, **13**, 1105–1130.. [Find this article online](#)
- Mariano, A. J., and O. Brown, 1992: Efficient objective analysis of heterogeneous and nonstationary fields via the parameter matrix. *Deep-Sea Res.*, **39**, 1255–1271..
- Orlic, M., M. Gacic, and P. E. La Violette, 1992: The currents and circulation of the Adriatic Sea. *Oceanol. Acta*, **15**, 109–124..

- Poulain, P.-M., 1999: Drifter observations of surface circulation in the Adriatic Sea between December 1994 and March 1996. *J. Mar. Syst.*, **20**, 231–253..
- , and P. Zanasca, 1998: Drifter and float observations in the Adriatic Sea (1994–1996). Data report, SACLANTCEN Memo. SM-340, 46 pp. [Available from SACLANT Undersea Research Centre, Viale San Bartolomeo 400, 19138 La Spezia, Italy.].
- , and —, 1999: Lagrangian measurements of surface currents in the northern and central Adriatic Sea. *The Adriatic Sea*, T. S. Hopkins et al., Eds., Ecosystems Research Rep. 32, Environment and Climate RTD Program of the European Commission, 107–115..
- Risken, H., 1989: *The Fokker-Planck Equation: Methods of Solutions and Applications*. Springer-Verlag, 472 pp..
- Smith, W. H. F., and D. T. Sandwell, 1997: Global sea floor topography from satellite altimetry and ship depth soundings. *Science*, **277**, 1956–1962..
- Swenson, M. S., and P. P. Niiler, 1996: Statistical analysis of the surface circulation of the California Current. *J. Geophys. Res.*, **101**, 22 631–22 646..
- Taylor, G. I., 1921: Diffusion by continuous movements. *Proc. London Math. Soc.*, **112**, 511–530..
- , 1953: Dispersion of soluble matter in solvent flowing slowly through a tube. *Proc. Roy. Soc. London*, **A219**, 186–283..
- Thomson, D. J., 1986: A random walk model of dispersion in turbulent flows and its application to dispersion in a valley. *Quart. J. Roy. Meteor. Soc.*, **112**, 511–530..
- , 1987: Criteria for the selection of stochastic models of particle trajectories in turbulent flows. *J. Fluid Mech.*, **180**, 529–556..
- Yeung, P. K., and S. B. Pope, 1989: Lagrangian statistics from direct numerical simulations of isotropic turbulence. *J. Fluid Mech.*, **207**, 531–586..
- Zambianchi, E., and A. Griffa, 1994: Effects of finite scales of turbulence on dispersion estimates. *J. Mar. Res.*, **52**, 129–148..
- Zore-Armanda, M., and M. Gacic, 1987: Effects of Bura on the circulation in the North Adriatic. *Ann. Geophys.*, **5B**, 93–102..

## APPENDIX A

### 7. Eddy–Mean Flow Decomposition Using an Optimized Spline

The method to compute optimized estimates of the mean flow  $U$  and of the turbulent parameters  $\sigma^2$ ,  $T_L$  from Lagrangian data using a spline interpolation is explained in [Bauer et al. \(1998\)](#). Here we briefly summarize some of the main aspects of the method.

A bicubic spline interpolation finite element procedure ([Inoue 1986](#)) is applied to sparse velocity data provided by Lagrangian instruments. The dataset is assumed to be stationary and the fluctuation statistics homogeneous over the region of interest. The spline results depend on four parameters: the value of knot spacing, which determines the number of finite elements, and three weights, associated with the uncertainties in the data and in the first and second derivatives. The parameters associated with the first and second derivatives are called tension and roughness, respectively. [Bauer et al. \(1998\)](#) showed that the knot spacing, the data weight, and the tension can be fixed a-priori, leaving only the roughness to be optimized. The tension is fixed to a high value (0.99 in a range between 0 and 1), to avoid rogue spike and anomalous behavior at the boundaries ([Inoue 1986](#); [Mariano and Brown 1992](#)). Regarding knot spacing and data weight, the choice of their value is not sensitive in a broad range once the roughness is left free to be optimized. Here we use a data weight proportional to the inverse of the estimated standard deviation of the eddy field, and a knot spacing of  $1^\circ$  (tests using  $0.5^\circ$  and  $0.25^\circ$  knot spacing show that the results are robust).

The roughness  $\rho$ , which controls the wavenumber content of the results, may attain values ranging between  $10^{-3}$  and  $10^3$ . The question is how to determine the optimal value of  $\rho$ , which provides the “best” estimates of  $U$ ,  $\sigma^2$ , and  $T_L$ . In [Bauer et al. \(1998\)](#) a criterion is proposed to define the best estimates, based on the minimization of a functional  $M(\mathbf{R}(\rho))$  which measures the distance of the autocovariance of the residual velocity,  $\mathbf{R}$ , from zero time lag up to timescales longer than the synoptic ones (i.e., typically longer than  $\approx 10$  days). Conceptually, this corresponds to a requirement of minimum energy in the fluctuation field for monthly and longer periods.

The application of the criterion to the Adriatic dataset suggests an optimal value of  $\rho = 100$ . The best  $U$  field, along with autocovariances and diffusivities, obtained for this value of  $\rho$  are shown in [Fig. 4a](#). As mentioned in [section 4](#), the diffusivity values are  $K_u \approx 1 \times 10^7 \text{ cm}^2 \text{ s}^{-1}$  and  $K_v \approx 3 \times 10^7 \text{ cm}^2 \text{ s}^{-1}$ .

A direct error estimate for this method is not straightforward. In [Bauer et al. \(1998\)](#) some indications have been obtained on the dependence of the errors on the number of independent observations,  $N_0$ , using Monte Carlo methods with a simplified stochastic model. The results are valid under the assumption of homogeneous and stationary statistics, so that they can be considered only as lower bounds for real data. For the results in [Fig. 4](#), obtained using the complete Adriatic dataset discussed in [section 2b](#), the total number of observation days is  $\sim 3900$ , which gives  $N_0 \sim 1300$  considering a timescale  $T_L \approx 1.5$  days. The results of [Bauer et al. \(1998\)](#) suggest a lower bound of 20% for the errors on  $U$  and  $K$ .

## APPENDIX B

### 8. Sensitivity to the Seasonality and to the Spatial Inhomogeneity of the Flow Regime

As mentioned in [section 4](#) and appendix A, the spline method for flow decomposition should in theory be applied to approximately stationary datasets, with homogeneous second-order moments. For the Adriatic dataset, this would require a partition of the data in time considering different seasons and in space considering smaller regions, for instance, separating boundary current regions from gyre interiors, characterized by markedly different eddy kinetic energy.

The present dataset is obviously not sufficient to characterize different temporal and/or spatial regimes: however, an attempt to use two different fields of  $U$  for winter and summer yielded for both seasons a value for  $K_u \approx 1 \times 10^7 \text{ cm}^2 \text{ s}^{-2}$ , that is, analogous to that obtained from the whole dataset; in contrast,  $K_v$  resulted  $\approx 2 \times 10^7 \text{ cm}^2 \text{ s}^{-2}$ , again for both seasons. As for the errors, they were estimated as discussed in [section 5](#), resulting  $>35\%$  for the summer data ( $N_0 \approx 450$ ) and  $>40\%$  for the winter data ( $N_0 \approx 300$ ), that is, within the error bracket for both seasons (see [Fig. 4](#)).

Since data are not sufficient to single out the boundary current regions, we have tried and isolated data corresponding to the southern basin. Again, the zonal diffusivity does not appreciably change, whereas  $K_v \approx 4 \times 10^7 \text{ cm}^2 \text{ s}^{-1}$ , with an error  $>26\%$  ( $N_0 \approx 800$ ), so that the difference again with the whole dataset falls within the error range.

In summary, the most sensitive parameter is the meridional diffusivity, which appears to vary between 2 and 4 ( $\times 10^7 \text{ cm}^2 \text{ s}^{-1}$ ). The variations cannot be considered significant with the present data density, even though they might suggest that  $K_v$  decreases when the seasonal fluctuations are properly resolved and  $K_v$  is higher in the southern basin.

## Tables

Table 1. Data relative to the “history” of drifters deployed in the Strait of Otranto between December 1994 and October 1995. Note that one of the drifters belonging to cluster 3 entered the Adriatic on 15 December 1995.

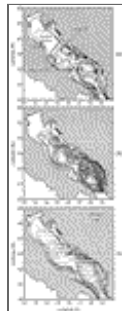
	Deployment		Crossing 40.4°N	
	Date	Number of drifters	Date	Number of drifters reaching north
Cluster 1	3 Dec 1994	7	13 Dec 1994–23 Jan 1995	4
Cluster 2	17–21 May 1995	15	24–31 May 1995	7
Cluster 3	22 July 1995	10	2–22 Aug 1995	3
Cluster 4	26–27 Aug 1995	10	29 Aug–1 Sep 1995	9
Cluster 5	13 Oct 1995	10	18–25 Oct 1995	8

[Click on thumbnail for full-sized image.](#)

Table 2. Comparison between data and model results as to number of drifters exiting the basin at  $t < 15$  days ( $n_S$ ); number of drifters reaching the northern Adriatic ( $n_N$ ); total number of drifters exiting the basin ( $n_T$ ); and average first exit time for the  $n_T$  drifters exiting from the basin ( $\langle AfT_1 \rangle$ ).

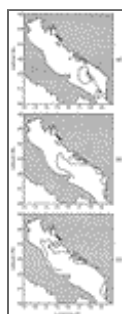
--	--

## Figures



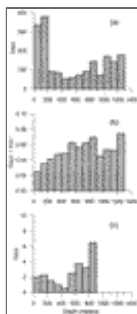
Click on thumbnail for full-sized image.

Fig. 1. (a) Bathymetric map of the Adriatic Sea with the subdivision proposed by [Artegiani et al. \(1997a\)](#); (b) trajectories of the surface drifters used in this study; (c) pseudo-Eulerian mean flow derived from the drifter data shown in (b) with a  $0.25^\circ$  by  $0.25^\circ$  binning (adapted from [Poulain 1999](#)).



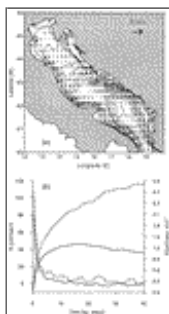
Click on thumbnail for full-sized image.

Fig. 2. Examples of individual drifter trajectories.



Click on thumbnail for full-sized image.

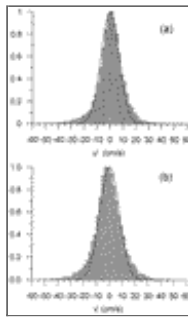
Fig. 3. (a) Distribution of bottom depths corresponding to drifter trajectories; (b) normalized distribution of bottom depths corresponding to drifter trajectories; (c) distribution of bottom depths corresponding to the drifters entering the Adriatic Sea by crossing  $40.4^\circ\text{N}$ .



Click on thumbnail for full-sized image.

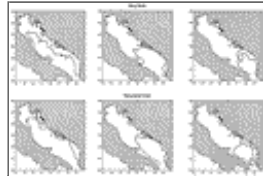
Fig. 4. (a) Large-scale mean flow  $U$  obtained by the bicubic spline technique; (b) autocovariances  $\mathbf{R}$  and diffusivities  $K$  resulting from the flow decomposition. Continuous (dotted) lines refer to the zonal (meridional) component.





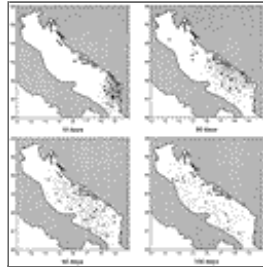
Click on thumbnail for full-sized image.

Fig. 5. Histograms of the fluctuating (turbulent) component of the velocity field,  $u'$  and  $v'$ .



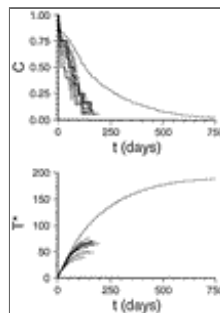
Click on thumbnail for full-sized image.

Fig. 6. Examples of real and simulated trajectories.



Click on thumbnail for full-sized image.

Fig. 7. Dispersion of simulated particles (smaller dots) and real drifters (bigger dots).



Click on thumbnail for full-sized image.

Fig. 8. Curves of normalized total tracer amount in the basin  $C(t)$  and tracer residence time  $T^*$ . Thin lines refer to simulation results, thick lines to data derived from the drifters.



© 2008 American Meteorological Society [Privacy Policy and Disclaimer](#)  
Headquarters: 45 Beacon Street Boston, MA 02108-3693  
DC Office: 1120 G Street, NW, Suite 800 Washington DC, 20005-3826  
[amsinfo@ametsoc.org](mailto:amsinfo@ametsoc.org) Phone: 617-227-2425 Fax: 617-742-8718  
[Allen Press, Inc.](#) assists in the online publication of *AMS* journals.

